JOINT INSTITUTE FOR NUCLEAR RESEARCH
Veksler and Baldin Laboratory of High Energy Physics

Electron Identification with MPD Experiment at NICA

Final Report of INTEREST Program

Student
Ayşe Sude Işık
Department of Science, Istanbul University
aysesude2814@gmail.com

Supervisor
Dr Sudhir Pandurang Rode
Veksler and Baldin Laboratory of High Energy Physics
sudhirrode11@gmail.com

Wave 11: November 05th – December 14th
Dubna 2024

Contents

Abstract

The MPD experiment, one of the flagship projects at the NICA accelerator complex in Dubna, is set to begin data taking in early 2026. To ensure the success of the experiment, it is crucial to optimize the performance of the MPD detector in event reconstruction, track reconstruction, and particle identification through detailed Monte Carlo simulations. This project specifically focuses on studying the electron identification capabilities of the MPD detector in Xe-Xe collisions under a 0.2T magnetic field. Sub-detectors such as the Time Projection Chamber (TPC), Time of Flight (TOF), and Electromagnetic Calorimeter (ECal) play key roles in this process. For example, the TPC allows for precise measurements of ionization loss (dE/dx), which helps differentiate electrons from other charged particles, while the TOF and ECal provide complementary information to refine identification. By learning and applying these simulation and reconstruction techniques, this study contributes to the broader goal of preparing the MPD experiment for reliable and accurate physics data analysis.

Keywords: Xe-Xe collisions, NICA, MPD detector, heavy-ion collisions, simulation.

1 Introduction

1.1 Introduction to High Energy and Heavy-Ion Physics

High energy and heavy-ion physics is a branch of physics dedicated to studying the fundamental properties of matter under extreme conditions. By recreating environments with high temperatures and densities, akin to those present in the early universe shortly after the Big Bang, researchers aim to explore Quantum Chromodynamics (QCD), the theory of strong interactions that govern the behavior of quarks and gluons. In such conditions, hadronic matter transitions into a state known as quark-gluon plasma (QGP), where quarks and gluons are no longer confined within hadrons. Studying QGP and other phenomena provides insights into the fundamental forces of nature and the evolution of the universe.

Studying QGP and associated phenomena provides crucial insight into the fundamental forces of nature, the structure of matter, and the evolution of the universe. The field also seeks to understand QCD phase transitions, the collective behavior of particles in dense nuclear mediums, and the mechanisms of particle production and decay in high-energy collisions. These objectives are pursued using large-scale accelerators capable of colliding particles at ultra-relativistic speeds, creating conditions where such phenomena can be observed.

1.2 The MPD Experiment at NICA

The Multi-Purpose Detector (MPD) is one of the cornerstone experiments at the newly developed Nuclotron-based Ion Collider fAcility (NICA) at the Joint Institute for Nuclear Research (JINR) in Dubna. NICA is designed to collide heavy ions at center-of-mass energies ranging from 4 to 11 GeV, an optimal regime for studying QCD matter at high baryonic densities and moderate temperatures. This complements the work of other facilities, such as the LHC and RHIC, which probe higher temperatures and lower baryonic densities. The MPD experiment is set to explore dense nuclear matter under extreme conditions, with a particular focus on investigating the QCD phase diagram and searching for the critical point that marks the transition between hadronic matter and QGP. By examining phenomena such as collective flow, particle correlations, and the dynamics of particle production, MPD will provide valuable data to advance our understanding of strong interactions. Scheduled to begin data collection in the early period of 2026, the experiment requires meticulous optimization of its detectors and simulation tools to ensure accurate reconstruction of collision events and the identification of particles with high precision.

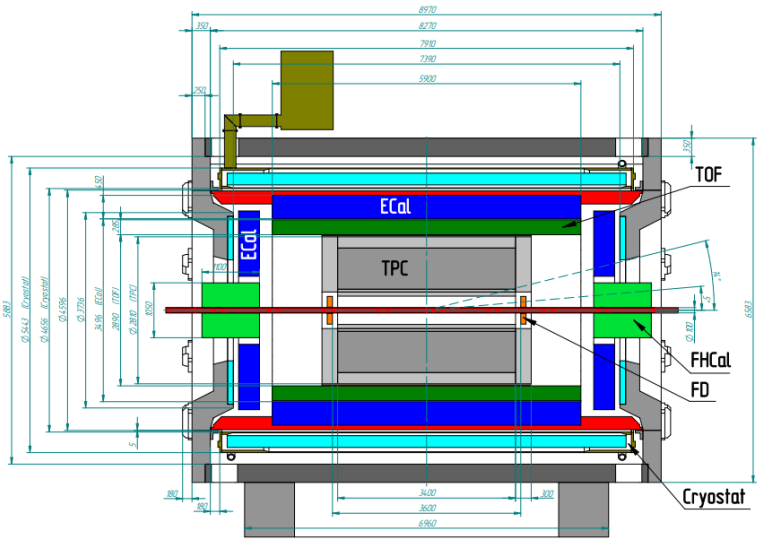

Figure 1: A vertical cross-sectional schematic of the MPD detector configuration for Stage 1.

An important distinction in some experimental setups, including specific test configurations, is the strength of the magnetic field used. Although the MPD TPC is designed to operate in a uniform magnetic field of 0.5T, my part of the project utilized a slightly reduced field strength of 0.2T. This difference in field strength has implications for the bending radius of charged-particle trajectories, which directly affects the resolution of momentum measurements and particle identification. A lower field strength should lead to less curvature for particles of a given momentum, potentially reducing the precision of momentum reconstruction, especially for high-momentum particles. However, with careful calibration and optimization of reconstruction algorithms, it is possible to maintain high performance even at 0.2T, demonstrating the flexibility and adaptability of the experimental setup.

1.3 MPD Sub-Detectors and Their Roles The MPD experiment employs a suite of advanced detector systems, including the Time Projection Chamber (TPC), Time-of-Flight (TOF) detector, and Electromagnetic Calorimeter (ECal), each designed to fulfill critical roles in tracking, particle identification, and energy measurement. The TPC serves as the primary tracking and particle identification detector, capable of reconstructing the trajectories of charged particles with high spatial resolution. When a charged particle traverses the gas-filled TPC, it ionizes the gas along its path, and the freed electrons drift under an electric field to a readout plane. By analyzing the arrival time and position of these electrons, the particle's 3D trajectory can be reconstructed. Additionally, the TPC measures the particle's specific ionization energy loss (dE/dx), which is velocity-dependent and provides a means to differentiate between particle species, such as electrons, pions, and kaons.

The TOF system of the MPD, developed for the identification of charged hadrons in the intermediate momentum range, is based on the technology of Multigap Resistive Plate Chambers (MRPC). The detector is designed to provide both time and coordinate measurements. By combining this time-of-flight data with the path length (obtained from the TPC) and momentum, the particle's velocity and mass can be calculated. This system is particularly effective at low and intermediate momenta, where it helps distinguish

between electrons and heavier hadrons. The TOF's high timing resolution enhances particle identification capabilities across a wide momentum range, especially when combined with the TPC's measurements.

The ECal plays a crucial role in identifying electrons and photons by measuring the energy they deposit while producing electromagnetic showers in a dense material. The primary role of the electromagnetic calorimeter is to measure, with good resolution, the spatial position and total deposited energy of electromagnetic cascades induced by electrons and photons produced in heavy ion collisions. The ECal will operate in the magnetic field of the MPD solenoid and will detect particles in the energy range from 10 MeV to a few GeV. The expected high multiplicity environment implies a high segmentation of the calorimeter. When high-energy electrons or photons interact with the ECal, they initiate a cascade of secondary particles that deposit energy proportional to the incident particle's energy. The ECal is designed to differentiate between electromagnetic and hadronic interactions, significantly reducing the background noise from hadrons and aiding in the precise identification of electrons. By rejecting particles that do not produce electromagnetic showers, ECal complements TPC and TOF in providing robust particle identification.

1.4 Electron Identification in the MPD Experiment Identifying electrons is a key component of the MPD experiment, as electrons serve as important probes for studying the properties of QGP and other QCD phenomena. Processes such as direct photon production, dilepton production, and the thermal radiation of the QGP often involve electrons, making their precise identification essential for extracting meaningful physics results. The identification process in MPD combines information from TPC, TOF, and ECal to achieve high precision. The TPC provides the first level of identification through dE/dx measurements, which allow for preliminary separation of electrons from other charged particles. The TOF further refines this identification by measuring the particles' velocities and isolating electrons at low and intermediate momenta where overlapping signals from heavier particles are common. Finally, the ECal confirms the presence of electrons by detecting their electromagnetic showers and rejecting nonelectromagnetic interactions, ensuring that hadronic contamination is minimized. An important aspect of particle behavior in heavy-ion collisions is the energy loss experienced by particles, especially partons (quarks and gluons) traversing the QGP. The energy loss of charged particles due to electromagnetic interactions can be described by the **Bethe-Bloch formula**:

$$\frac{dE}{dx} = \frac{4\pi z^2 e^4}{m_e c^2 \beta^2} \left(\ln \left(\frac{2 m_e c^2 \beta^2}{I} \right) - \beta^2 \right)$$

where: - $\frac{dE}{dx}$ is the rate of energy loss per unit length, - z is the charge of the particle, - e is the elementary charge, - m_e is the electron mass, - c is the speed of light, - $\beta = \frac{v}{c}$ is the velocity of the particle relative to the speed of light, - I is the mean excitation energy of the medium. We will analyze the data obtained from our experiment, with a particular focus on the energy loss per unit distance ($\frac{dE}{dx}$) for electron identification. This detailed examination of the $\frac{dE}{dx}$ distribution is essential for distinguishing electrons from other particle types based on their characteristic energy loss patterns in the detector material.

Reconstruction and simulation play a critical role in the electron identification process. Using Monte Carlo simulations, realistic collision events are generated on the basis

of theoretical models. These simulations propagate particles through the detector geometry and simulate their interactions, energy losses, and signals in each subsystem. By comparing simulated and experimental data, the performance of the detectors and reconstruction algorithms can be optimized. Reconstruction procedures involve associating signals from the TPC, TOF, and ECal to individual particles, accurately identifying their properties, and extracting key physics parameters.

2 Project Objectives

Study of electron identification capability of MPD detector using various sub-detectors such as Time Projection Chamber (TPC), Time of flight (TOF) detector and Electromagnetic Calorimeter (ECal) by means of various detection techniques such as ionization loss (dE/dx) measurements in the TPC.

3 Methodology

3.1 Simulation This study focuses on the identification of electrons in Xe-Xe collisions using the MPD detector at the NICA accelerator complex. The process involves event generation, detector simulation, event reconstruction, data analysis, and parametrization.

To simulate the Xe-Xe collisions, the Ultra-relativistic Quantum Molecular Dynamics (UrQMD) model was employed. This model is widely used in heavy-ion physics for generating realistic particle production in high-energy collisions. The collisions involved Xe-Xe nuclei with an atomic number $Z = 54$ and mass number $A = 124$. A total of 100,000 events were generated to ensure statistical significance, with the impact parameter set between 0 and 16 fm to encompass a broad range of collision centralities. The generated events included all final-state particles and their kinematic properties, such as momentum, energy, and particle type.

```
#do not decay K*
sth 108
sth -108
#do not decay K*0
sth 110
sth -110
#do not decay Lambda*
sth 29
sth -29
#do not decay Sigma*
sth 41
sth -41
#do not decay Xi*
sth 50
sth -50

f13
#f14
f15
f16
f19
f20

xxx
```

(a) Input details for event generation.

```
pro 124 54
tar 124 54

nev 100000
imp -16

ecn 7
tin 200 200
eos 0
rsd 11

#do not decay pi
sth 101
#do not decay eta
sth 102
#do not decay omega
sth 103
#do not decay rho
sth 104
#do not decay eta-prime
sth 107
#do not decay phi
sth 109
#do not decay K*
```

(b) Input details for event generation.

Figure 2: Overall caption for the two figures.

The generated events were subsequently propagated through a detailed simulation of the MPD detector using the MPDROOT framework, which is based on FairRoot.

Key sub-detectors—namely the Time Projection Chamber (TPC), Time-of-Flight (TOF) detector, and Electromagnetic Calorimeter (ECal)—were modeled in the simulation. The TPC simulated ionization losses (dE/dx) to provide initial particle identification, while the TOF calculated time-of-flight information to determine particle velocity and mass. The ECal simulated energy deposition and electromagnetic shower formation to aid in the identification of electrons and photons. The simulations were performed under a magnetic field of 0.2 T, a configuration chosen to reflect realistic conditions while studying its implications for momentum resolution.

Reconstruction of simulated data was performed using MPDROOT's built-in algorithms. Tracks were reconstructed using hits recorded in the TPC, TOF, and ECal. Signals from these detectors were matched to associate them with individual particles, and key properties such as momentum, energy, and particle identification likelihood were calculated. To ensure the reliability of the results, calibration parameters, including detector alignment and signal response, were optimized to reduce reconstruction errors and enhance identification accuracy.

3.2 Analysis Techniques Custom analysis codes were written to extract and study electron-specific properties from the reconstructed data. Variables such as dE/dx, velocity, and energy deposition were visualized as histograms for electrons and background particles.

```
// MPD includes
#include "TpcPoint.h"
#include "MpdTpcKalmanTrack.h"
#include "MpdKalmanFilter.h"
#include "MpdKfV0Fitter.h"
#include "MpdTofMatching.h"
#include "MpdEvent.h"
#include "MpdTrack.h"
#include "MpdEventHeader.h"
#include "BaseTpcSectorGeo.h"
```

(a) MPD classes that were used for the Analysis.

```
// CBM includes
#include "FairEventHeader.h"
#include "FairMCPoint.h"
#include "MpdMCTrack.h"
#include "FairRunAna.h"
#include "FairRuntimeDb.h"
#include "FairParRootFileIo.h"
```

(b) FAIR classes that were used for the Analysis.

Figure 3: Directories for the analysis codes.

These distributions were fitted(Fig. 4) with appropriate functions, such as Gaussian, to obtain mean (μ) and standard deviation (σ) values. To separate electrons from other particles, such as pions and kaons, selection criteria were applied based on the dE/dx measurements in the TPC, TOF timing, and ECal energy deposition. Statistical techniques were employed to calculate electron purity and efficiency within the sample.

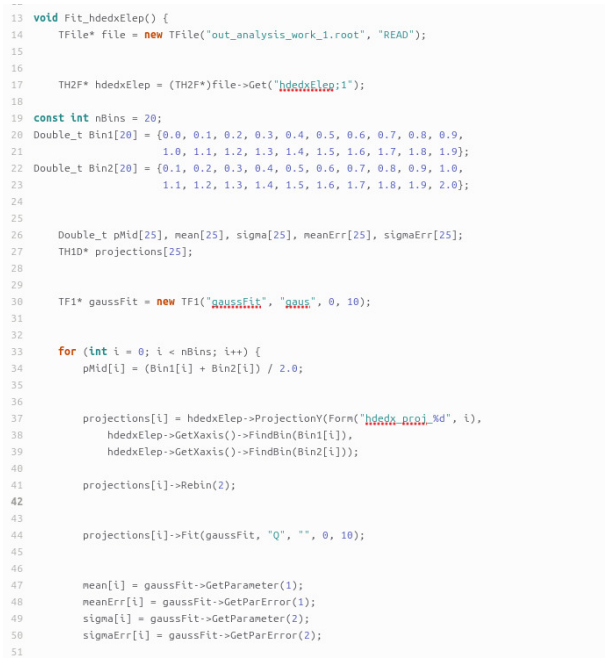

```
void Fit_hdedxElep() {
    TFile* file = new TFile("out_analysis_work_1.root", "READ");


    TH2F* hdedxElep = (TH2F*)file->Get("hdedxElep;1");

const int nBins = 20;
Double_t Bin1[20] = {0.0, 0.1, 0.2, 0.3, 0.4, 0.5, 0.6, 0.7, 0.8, 0.9,
                     1.0, 1.1, 1.2, 1.3, 1.4, 1.5, 1.6, 1.7, 1.8, 1.9};
Double_t Bin2[20] = {0.1, 0.2, 0.3, 0.4, 0.5, 0.6, 0.7, 0.8, 0.9, 1.0,
                     1.1, 1.2, 1.3, 1.4, 1.5, 1.6, 1.7, 1.8, 1.9, 2.0};


    Double_t pMid[25], mean[25], sigma[25], meanErr[25], sigmaErr[25];
    TH1D* projections[25];


    TF1* gaussFit = new TF1("gaussFit", "gaus", 0, 10);


    for (int i = 0; i < nBins; i++) {
        pMid[i] = (Bin1[i] + Bin2[i]) / 2.0;


        projections[i] = hdedxElep->ProjectionY(Form("hdedx proj %d", i),
            hdedxElep->GetXaxis()->FindBin(Bin1[i]),
            hdedxElep->GetXaxis()->FindBin(Bin2[i]));

        projections[i]->Rebin(2);


        projections[i]->Fit(gaussFit, "Q", "", 0, 10);


        mean[i] = gaussFit->GetParameter(1);
        meanErr[i] = gaussFit->GetParError(1);
        sigma[i] = gaussFit->GetParameter(2);
        sigmaErr[i] = gaussFit->GetParError(2);

```

Figure 4: Example fitting code for the histograms obtained from the analysis code.

Parametrization(Fig. 5) was carried out to generalize the detector's response across different kinematic ranges. The mean (μ) and sigma (σ) values obtained from the fitted histograms were parameterized as functions of momentum or other kinematic variables. Analytical functions, such as polynomials, were used, and the fits were refined iteratively to minimize residuals and ensure accuracy. The parameterized functions were validated by comparing them to the original data, confirming their consistency and reliability.

```
if (TMath::Abs(mpdTrack->GetEta()) < 1.0) {// acceptance
      if (TMath::Abs(mcTr->GetPdgCode()) == 11 && pd < 2) hAllEleRecDen->Fill(mcTr->GetPt());
      if (mpdTrack->GetNofHits() > 20) {// number of hits
        if (TMath::Abs(mcTr->GetPdgCode()) == 11 && pd < 2) hAllEleRecHits->Fill(tr->Pt());// effi numerator 1
        if (abs(DCAx_Sig_out) < 3 && abs(DCAy_Sig_out) < 3 && abs(DCAz_Sig_out) < 3) {// DCA cut 3
        hDCAx_vs_Pt->Fill(tr->Pt(), DCAx_Sig_out);
        hDCAy_vs_Pt->Fill(tr->Pt(), DCAy_Sig_out);
        hDCAz_vs_Pt->Fill(tr->Pt(), DCAz_Sig_out);
          if (TMath::Abs(mcTr->GetPdgCode()) == 11 && pd < 2) hAllEleRecDCA->Fill(tr->Pt());// effi numerator 2
          if (abs(dedxsigma_npd) < 2.0) {// dedx 1
              hDedxSigma_vs_Pt->Fill(tr->Pt(), dedxsigma_npd);
              hAllTPC->Fill(tr->Momentum());// purity tpc denominator
               if (TMath::Abs(mcTr->GetPdgCode()) == 11) hEleTPC->Fill(tr->Momentum());//purity tpc numerator
            if (TMath::Abs(mcTr->GetPdgCode()) == 11 && pd < 2) hAllEleRecTPC->Fill(tr->Pt());// effi numerator 3
            if (abs(TOFmatchingdphi_sigma) < 2 && abs(TOFmatchingdz_sigma) < 2) {// TOF matching dphi and dz 2
            hTOFdphi_vs_Pt->Fill(tr->Pt(), TOFmatchingdphi_sigma);
            hTOFdz_vs_Pt->Fill(tr->Pt(), TOFmatchingdz_sigma);
              if (TMath::Abs(mcTr->GetPdgCode()) == 11 && pd < 2) hAllEleRecTPCTOFMatch->Fill(tr->Pt());// effi numerator 4
              if (TMath::Abs(betasigma_npd) < 2) {//tof pid 1
                htofpid->Fill(tr->Momentum(), tr->GetBeta());
                hall->Fill(tr->Momentum());//purity tpc+tof denominator
                if (TMath::Abs(mcTr->GetPdgCode()) == 11) hEle->Fill(tr->Momentum());//purity tpc+tof numerator
                if (TMath::Abs(mcTr->GetPdgCode()) == 11 && pd < 2) hAllEleRecTPCTOF->Fill(tr->Pt());// effi numerator 5
                 if (abs(Ecalmatchingdphi_sigma) < 2 && abs(Ecalmatchingdz_sigma) < 2) {// ecal matching dphi and dz 2
                 hEcaldphi_vs_Pt->Fill(tr->Pt(), Ecalmatchingdphi_sigma);
                 hEcaldz_vs_Pt->Fill(tr->Pt(), Ecalmatchingdz_sigma);
                   if (TMath::Abs(mcTr->GetPdgCode()) == 11 && pd < 2) hAllEleRecTPCTOFECalMatch->Fill(tr->Pt());// effi numerator 6
                   if (Ep_cut_nsigma == 1) {// ecal PID E/p 1
                     hecalpid->Fill(tr->Momentum(), tr->GetDedx());
                      hEpCutNsigma_vs_Pt->Fill(tr->Pt());
                      hAllECal->Fill(tr->Momentum());// purity ecal denominator
                      if (TMath::Abs(mcTr->GetPdgCode()) == 11) hEleECal->Fill(tr->Momentum());//purity ecal numerator
                      if (TMath::Abs(mcTr->GetPdgCode()) == 11 && pd < 2) hAllEleRecTPCTOFECalPID->Fill(tr->Pt());// effi numerator 7
```

Figure 5: Applying cuts and parameterize the data according our fits.

This methodology combines advanced simulation, reconstruction, and analysis techniques to study electron identification in Xe-Xe collisions. With the help of complementary strengths of the TPC, TOF, and ECal subsystems, along with robust statistical methods, ensures a high level of accuracy in electron identification and provides a strong foundation for future experimental data analysis.

4 Results

4.1 DCA (Distance of the Closest Approach) Plots These plots represent the x, y, and z components of the Distance of Closest Approach (DCA) between the reconstructed particle trajectory and the primary collision vertex. A smaller DCA indicates that the particle likely originated from the primary collision rather than a secondary process.

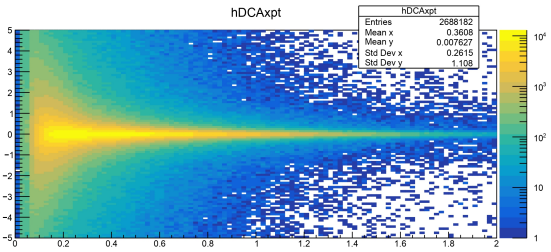

Figure 6: DCA-X/p_T

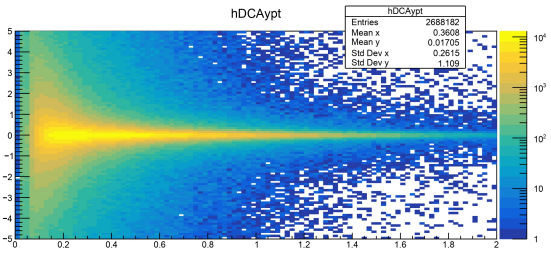

Figure 7: DCA-Y/p_T

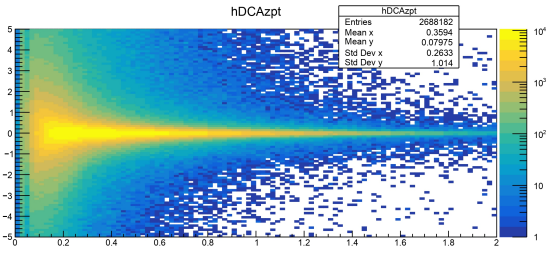

Figure 8: DCA-Z/p_T

4.2 Specific Ionization Energy Loss(de/dx) Plot The specific ionization energy loss (dE/dx) measures how electrons lose energy as they traverse the gas in the Time Projection Chamber (TPC). This variable helps distinguish electrons from heavier particles like protons and kaons, especially at low momenta.

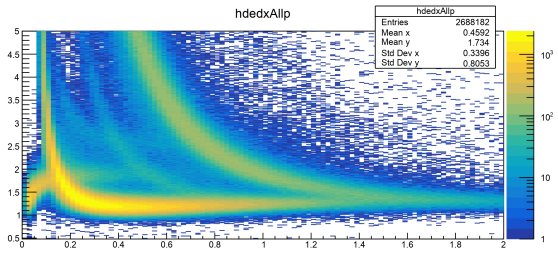

Figure 9: $(dE/dx)/p$: Specific Ionization Energy Loss

4.3 Complementary Plots for Further Analysis These plots show the matching of TPC tracks to TOF signals using azimuthal angle ($\Delta\phi$) and longitudinal displacement (Δz) differences. Narrow peaks centered around zero indicate effective matching.

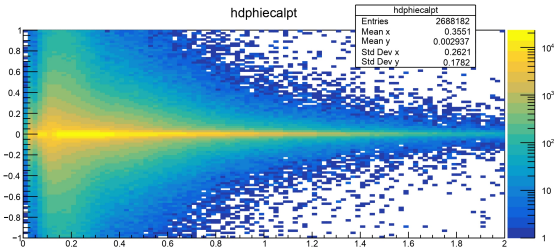

Figure 10: $d\phi/p_T$: Azimuthal Matching in TOF

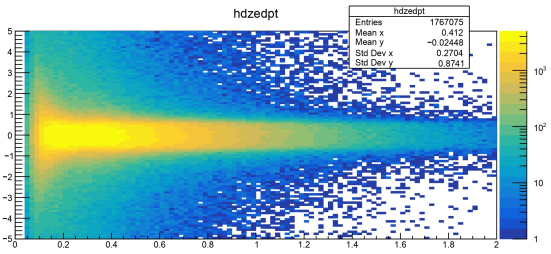

Figure 11: dz/p_T: Longitudinal Matching in TOF

This (Fig. 12) plot presents the relationship between the Time of Flight (TOF) beta measurement and particle momentum. This plot is essential for understanding how particle velocity varies with momentum, offering insights into the separation of different particle species. The beta distribution provides a foundation for distinguishing between particles such as electrons, protons, and pions based on their TOF measurements.

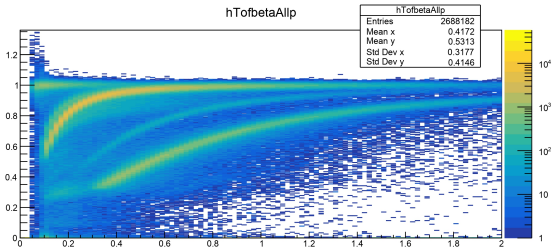

Figure 12: β (Velocity as v/c) for Electrons in TOF

This plot (Fig. 13) shows the energy-to-momentum ratio (E/p) for particles interacting with the Electromagnetic Calorimeter (ECal). Electrons, which deposit nearly all their energy in electromagnetic showers, should exhibit $E/p \approx 1$.

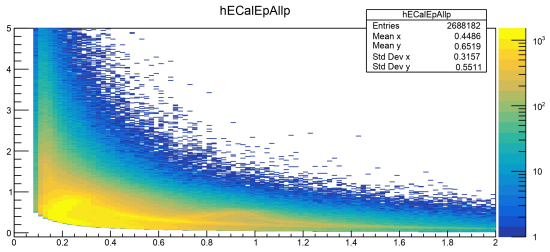

Figure 13: E/p: Energy-to-Momentum Ratio for ECal

These plots examine the matching of TPC tracks to ECal signals using $\Delta\phi$ and Δz. Narrow peaks at zero confirm successful matching.

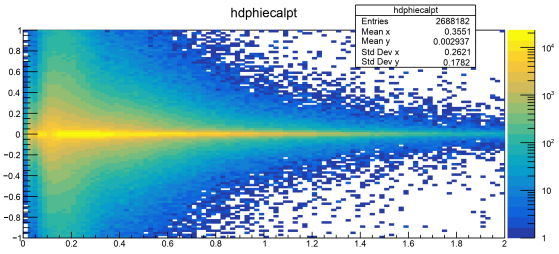

Figure 14: $d\phi/p_T$: Azimuthal Matching in ECal

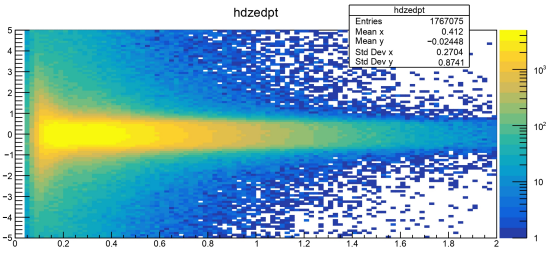

Figure 15: dz/p_T: Longitudinal Matching in ECal

4.4 Efficiency and Purity Plots

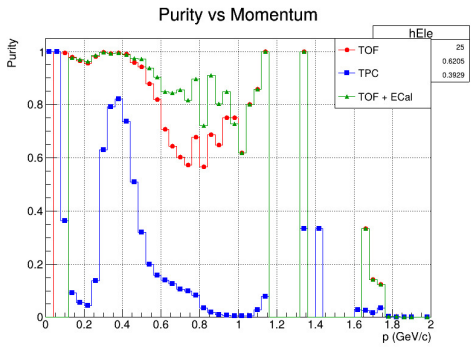

(a) Purity analysis.

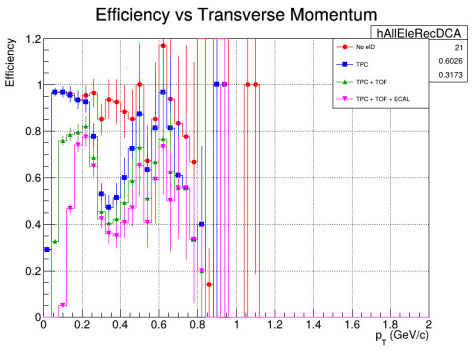

(b) Efficiency analysis.

Figure 16: Directories for the analysis codes.

The Electromagnetic Calorimeter (ECal) plays a critical role in separating hadrons from electrons, especially at high momentum. This capability is particularly important as it ensures that the selected sample remains uncontaminated by misidentified particles. Using the distinct responses of hadrons and electrons in the ECal, the purity of the selected events can be significantly improved, which is essential for maintaining the accuracy of the analysis. (Fig. 16-a)
For a uniform shape of the efficiency curve, optimization of the parametrization is required. This involves refining the selection criteria to ensure consistent performance across the relevant ranges, such as energy or momentum. Additionally, more statistics are needed to reduce fluctuations and improve the reliability of the efficiency plots. A smooth efficiency curve not only reflects the stability of the analysis but also enhances the confidence in interpreting the detector's performance. (Fig. 16-b)

5 Discussion

The presented plots offer a detailed overview of the detector's performance and its effectiveness in particle identification, particularly for electrons. The x, y, and z components of the Distance of Closest Approach (DCA) reveal the precision of track reconstruction and highlight the ability to distinguish primary particles originating from the collision vertex. Tightly centered distributions around zero confirm the effectiveness of vertex reconstruction, while broader deviations may indicate contamination from secondary particles or systematic biases. The dE/dx measurements in the Time Projection Chamber (TPC) demonstrate clear separation between electrons and heavier particles at low momenta, where ionization losses differ significantly. This separation is further refined by the application of Time-of-Flight (TOF) and ECal cuts, as evident from the enhanced dE/dx distributions. The TOF matching parameters, $\Delta\phi$ and Δz, show well-constrained alignment of TPC tracks with TOF signals, reinforcing the accuracy of the particle tracking and timing systems. Furthermore, the β values obtained from TOF confirm the ultrarelativistic nature of the identified electrons, consistent with theoretical expectations. The energy-to-momentum ratio (E/p) derived from the Electromagnetic Calorimeter (ECal) measurements highlights the detector's capability to identify electrons with high efficiency, as electrons deposit nearly all their energy in the calorimeter. Also for these

plots different bands are suggesting different particle responses. Matching parameters between the TPC tracks and ECal signals, such as $\Delta\phi$ and Δz, further demonstrate precise reconstruction, ensuring minimal contamination from mismatched tracks.

6 Conclusion

Overall, the results validate the robustness of the combined detector systems, with each component contributing to the reliable identification of electrons. These findings confirm the high performance of the detector in delivering accurate measurements, forming a solid foundation for subsequent physics analyzes. However, further optimization might be necessary to account for potential systematic effects, such as regional variations in detector response or momentum-dependent biases. Future efforts could also explore advanced techniques, including machine learning-based particle identification, to enhance the resolution and efficiency of the analysis. Incorporating more statistics will help refine the analysis results, especially in terms of efficiency and purity, where some imperfections are currently observed. By increasing the statistics, we can reduce statistical fluctuations and achieve more reliable and consistent results. Additionally, optimizing the cuts in parametrization and selection criteria will further improve the precision of the analysis, allowing for clearer separation of particle types and better overall performance in both efficiency and purity plots. More precise cuts, combined with a larger statistical sample, will lead to a more accurate and robust analysis.

Acknowledgements

I would like to express my heartfelt gratitude to my supervisor, Dr. Sudhir Pandurang Rode. He is one of the best educators I have had the privilege of learning from. His constant availability, patience, and invaluable guidance were instrumental in helping me complete this project. Moreover, his support has enriched my understanding and significantly contributed to my growth as a physicist. I will always be deeply grateful for his contributions to my learning journey. I would also like to express my heartfelt thanks to my project friend, Rishav, for their invaluable experience in the Interest projects.

References

1. Status and initial physics performance studies of the MPD experiment at NICA
2. Relativistic Kinematics by R. Sahoo
3. Three Stages of the NICA Accelerator Complex
4. MPD ROOT Guide